

September 2020

**Keywords or phrases:**

Metabolism, Cancer Metabolism, ATP, Metabolic Requirements, Glycolysis, Glucose, Cancer, Metabolic-Symbiosis

# Incucyte<sup>®</sup> ATP Assay Enables Direct, Live-Cell Measurement of ATP

## Introduction

Altered tumor cell metabolism was first observed over a hundred years ago. Since then, metabolic reprogramming has been firmly established as a hallmark of cancer, and the means by which it supports the increased energetic, biosynthetic, and redox demands associated with tumor development and progression have been extensively investigated<sup>1</sup>. Studies across a variety of tumor types have demonstrated that dependence on glucose and glutamine are amongst the common metabolic requirements of cancer cells, both of which can be utilized to fuel production of ATP, the fundamental molecule for energy storage and transfer at the cellular level. Researchers are actively investigating ways to exploit these and other metabolic vulnerabilities for therapeutic purposes.

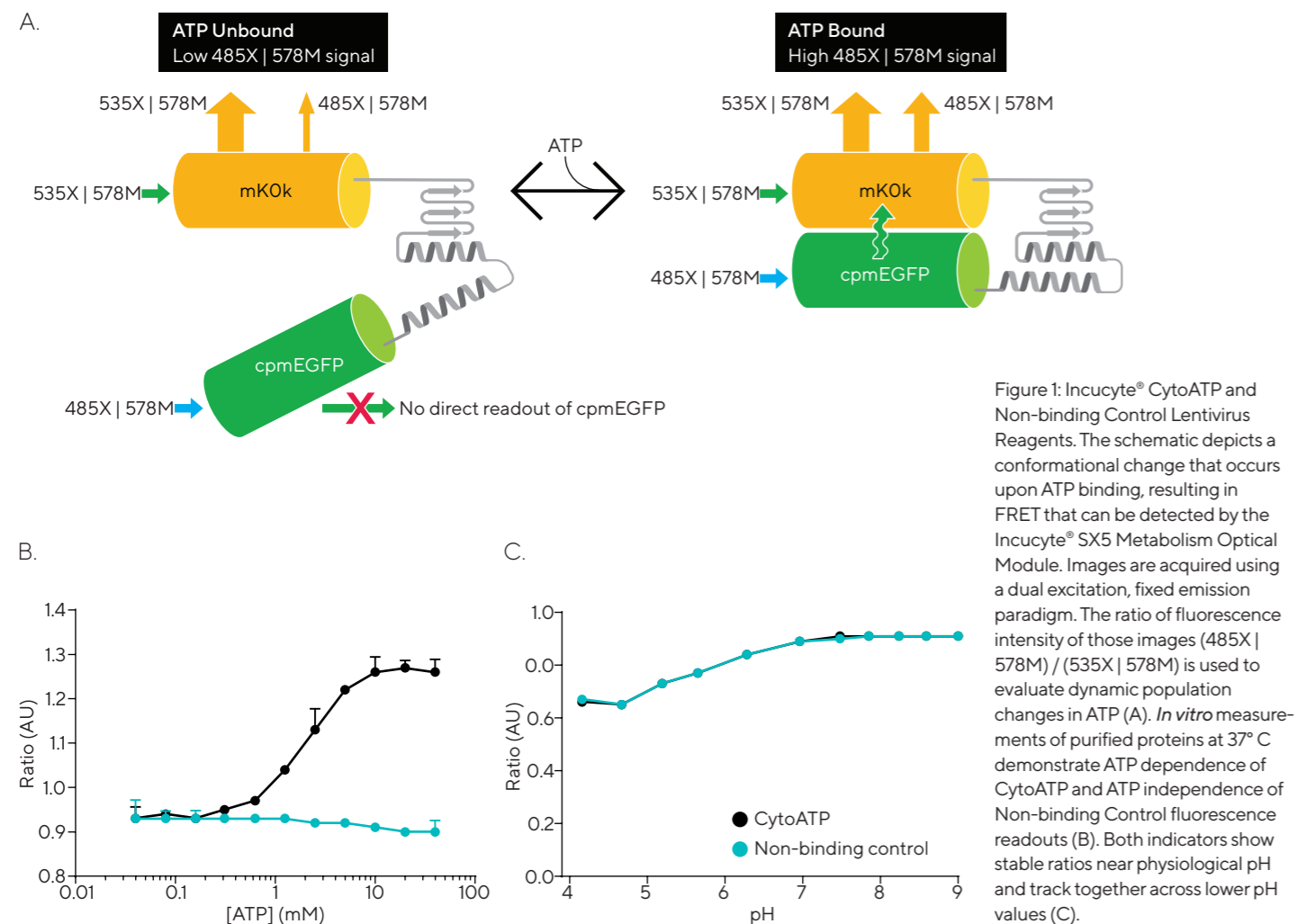
Standard approaches to studying perturbations of ATP and other metabolites rely on endpoint assays that provide limited kinetic information and lack cell-specific data in co-culture models. These assays are also often destructive, prohibiting qualitative visual assessment of morphological changes associated with metabolic perturbations. Because nutrient exchange between tumor and stromal cells can mediate resistance to metabolically-targeted treatments<sup>2</sup>, technologies that enable direct monitoring of metabolic readouts in co-culture models are critical for the advancement of such therapeutics. Live-cell analysis holds promise for greater physiological relevance and insight by providing the necessary tools to study cell-specific metabolic readouts and morphology in mono- or co-culture over time without the need for repeated end point measurements. In this application note, we describe the development and utility of the Incucyte<sup>®</sup> ATP Assay, encompassing novel reagents and purpose-built instrumentation and analytical tools created with these needs in mind.

## Assay Principle

The Incucyte® CytoATP Lentivirus Kit has been developed to enable non-perturbing measurement of dynamic changes in cytoplasmic ATP. The kit contains a set of two live-cell reagents, encoding ATP-binding (CytoATP Lentivirus) and ATP nonbinding (CytoATP Non-binding Control Lentivirus) indicators. Both are single cassette, dual fluorescent reporters comprised of cpmEGFP and mKOκ tethered by an ATP binding domain, identical except for the introduction of two mutations that prevent ATP binding in the Non-binding Control. Inclusion of CytoATP Non-binding Control in live-cell assays enables calculation of the Corrected ATP Ratio, thereby minimizing contribution of experimental artifacts that may affect fluorescence output (e.g., pH) and setting a limit of detection.

Figure 1A illustrates the principle of the CytoATP reagent. Upon ATP binding, a conformational change brings the two fluorescent proteins closer together, thereby increasing the efficiency of Förster resonance energy transfer (FRET) from donor (cpmEGFP) to acceptor (mKOκ). These changes can be detected using the Incucyte® SX5 Metabolism Optical Module, which utilizes a dual excitation and fixed, single

emission acquisition strategy. ATP-dependent changes in fluorescence are incorporated in the 485X | 578M readout, and reporter expression is reflected in the direct excitation and emission of mKOκ (535X | 578M). The purpose-built Incucyte® ATP Analysis Software Module calculates the ratio of fluorescence intensity of those images (485X | 578M) / (535X | 578M) to enable direct measurement of ATP independent of cell number or indicator expression levels (Figure 1A). To characterize the binding of CytoATP to ATP, the fluorescence emission ratio of the purified protein was measured using a plate reader. A linear increase in the fluorescence emission ratio of CytoATP was observed across a physiological range of ATP<sup>3</sup> (K<sub>d</sub> = 2.2 mM at 37° C). In contrast, the output of purified Non-binding Control protein was unaffected by the presence of up to 40 mM ATP (Figure 1B). In the absence of ATP, the ratiometric fluorescence signal for both indicators was overlapping across a range of pH. Both reporters demonstrated a stable fluorescence ratio within the cytosolic physiological range of pH. A decrease in ratio was observed at lower pH values, with both displaying identical changes across all values (Figure 1C).



## Materials and Methods

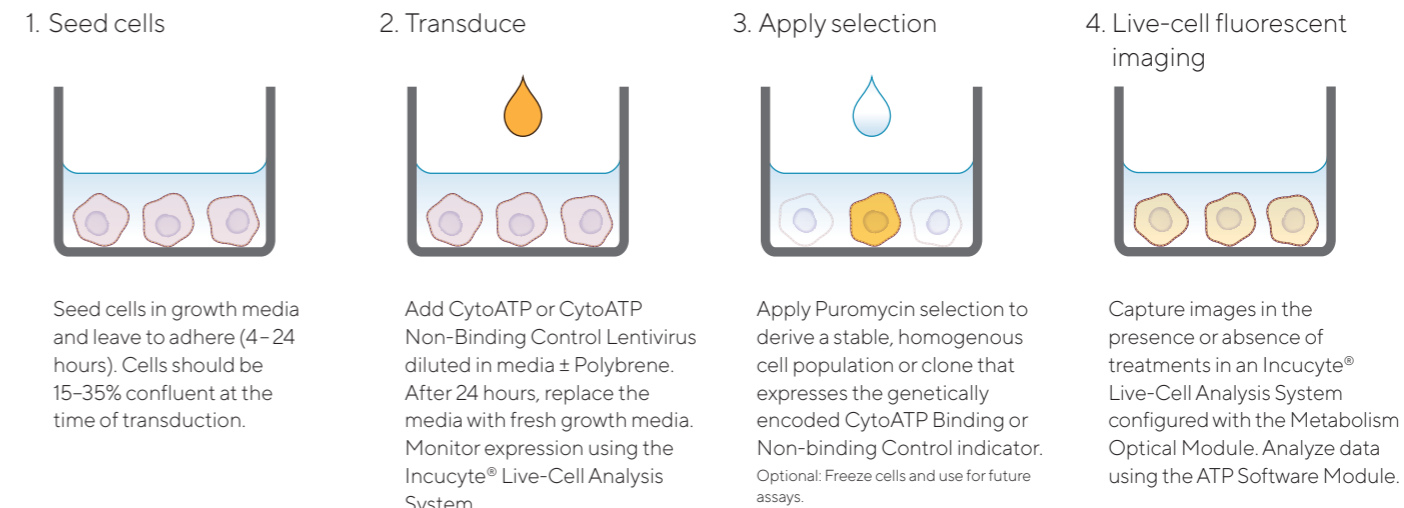


Figure 2: Quick guide for generating cell lines stably expressing Incucyte® CytoATP or Non-binding Control indicators.

The CytoATP Lentivirus Reagent Kit was utilized to generate cell lines stably expressing CytoATP and Non-binding Control indicators<sup>4</sup>. Multiplicity of Infection (MOI) was optimized for each cell line using the Incucyte® SX5 Live-Cell Analysis System to monitor expression and cell health. After cells were allowed to recover and achieve suitable expression levels, puromycin selection was applied to remove non-expressing cells. Growth curves and morphology of stably transduced cell lines were comparable with their corresponding parental cell lines across all cell types evaluated (data not shown). All live-cell ATP experiments were performed utilizing an Incucyte® SX5 configured with an Incucyte® Metabolism Optical Module, and images were acquired and analyzed using the Incucyte® ATP Analysis Software Module.

### CellTiter-Glo® ATP Assay

A549 cells stably expressing CytoATP indicators were plated at 4,000 cells/well or 8,000 cells/well in a 96-well microplate. After overnight incubation, cells were treated with compounds and monitored in the Incucyte® ATP assay as described below. Two hours after compound treatment, the same plate of cells was used to perform a CellTiter-Glo® (CTG) ATP assay (Promega) according to manufacturer instructions. CTG luminescence measurements were performed using a FlexStation II plate reader (Molecular Devices).

### Protein Characterization

Fluorescence emission of CytoATP and Non-binding Control purified proteins (0.5 μM final concentration) was measured at the fixed emission wavelength of 590 nm while exciting at 488 nm or 551 nm. Indicator response was calculated as a ratio of the fluorescence emission measured at ex = 488 nm to that measured at ex = 551 nm. All measurements were performed in a 96-well plate using a Spark plate reader (Tecan) at 37° C. To evaluate ATP-dependence, measurements were performed in PBS with varying concentrations of Mg-ATP (equimolar mix of ATP and MgCl<sub>2</sub>). To evaluate pH dependence, measurements were performed in buffers with varied pH and in the absence of ATP.

## Live-Cell Analysis of ATP Modulation

Cellular ATP is generated via two pathways, glycolysis and oxidative phosphorylation (OXPHOS). Concurrent pharmacological blockade of these two synthetic pathways was performed in order to verify the ability of the Incucyte® ATP Assay to track dynamic changes in ATP in live cells. A549 cells stably expressing CytoATP indicators were treated with a combination of 2-Deoxy-D-glucose (2-DG, 0.6–40 mM), which blocks glycolysis through competitive inhibition of hexokinase<sup>5</sup>, and potassium cyanide (KCN, 0.06–4 mM), which acts at mitochondrial cytochrome c oxidase to inhibit OXPHOS<sup>6</sup>. Images were acquired and analyzed every 20 min in dual excitation, single emission Ratio Mode as described above. Two baseline scans were performed to demonstrate that prior to compound addition, all wells showed comparable fluorescence ratios. Utilizing the Incucyte® ATP Analysis Software Module, images can be segmented based on 535X | 578M fluorescence, representative of total protein expression (yellow outlines, Figure 3A). This segmentation mask is automatically used to analyze 485X | 578M fluorescence. The direct ratio of fluorescence intensity measured from those two images (485X | 578M) / (535X | 578M) is used to calculate ATP Ratio metrics as a measure of relative ATP level.

As shown in Figure 3B, a concentration-dependent depletion of ATP occurs very rapidly following combined 2-DG and KCN treatment, with the highest concentrations dropping ATP to near the limit of detection, equal to 0 when plotting Corrected ATP Ratio, within 20 min of administration. A small and transient increase in CytoATP readout is observed at the first time point after treatment due to a temperature-dependent decrease in Kd of CytoATP. Treatment-induced effects on ATP can also be visualized by color-scaled ratio images within the Incucyte® ATP Software. Cells in vehicle-treated wells at the top of the plate appear bright yellow, while the lower ATP levels of cells treated with 2-DG + KCN are reflected as progressively dimmer yellow as concentrations increase down the plate (Figure 3C). Similar responses were observed across all seventeen cell lines tested (data not shown). These data demonstrate the ability of CytoATP reporters to provide direct, live-cell measurements of rapid changes in ATP.

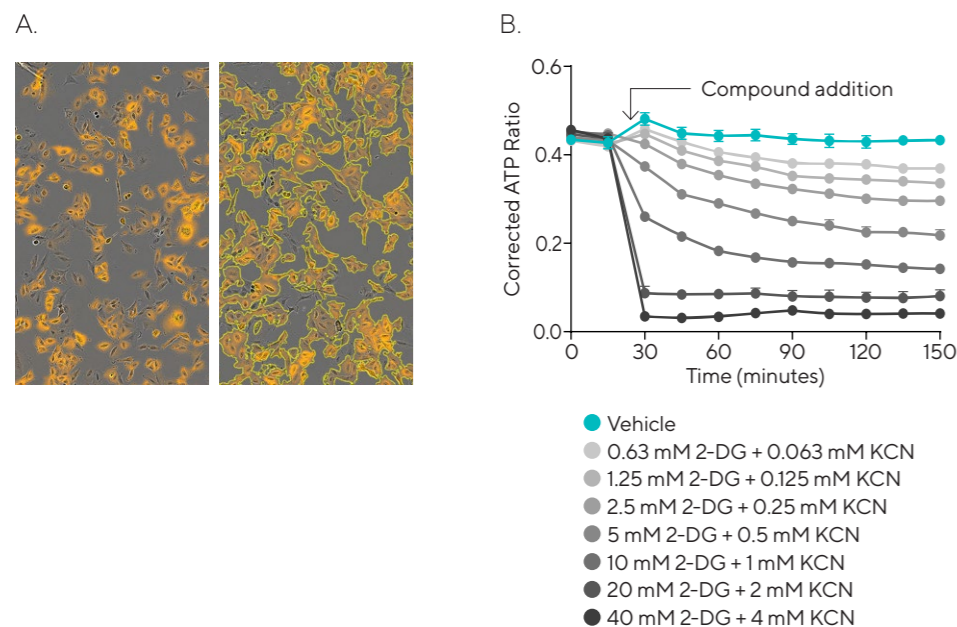


Figure 3: Direct measurement of ATP in live cells. Images of A549 cells stably expressing Incucyte® CytoATP indicators are segmented (yellow outlines, right half of image) based on 535X | 578M fluorescence (A). Analysis demonstrates a rapid, concentration-dependent decrease in ATP following combined 2-DG and KCN treatment blockade of glycolysis and OXPHOS, respectively (B). Color-scaled ratio images provide visualization of concentration-dependent ATP depletion in cells treated with 2-DG + KCN compared to vehicle (C).

## Measurement of ATP Independent of Cell Number

Many standard metabolic assays provide measurements of mass, consumption rates, or other such parameters which are cell-number dependent. Because metabolic perturbations can rapidly alter cell growth, the need for a separate assay to account for differences in cell number is often a critical aspect of the experimental workflow to ensure appropriate interpretation of data. A unique feature of the CytoATP reagent is the ability to provide direct, ratiometric ATP measurements independent of cell number or indicator expression level.

To demonstrate this concept, HeLa cells stably expressing CytoATP or Non-binding Control reporters were seeded at 4,000 cells/well and 8,000 cells/well in a 96-well microplate and exposed to combined 2-DG (0.6–40 mM) and KCN (0.06–4 mM) treatment to induce ATP depletion. Compound effects were monitored continuously over the next 2 h using the Incucyte® ATP assay. In a separate study, CTG measurements were confirmed to be comparable between parental cells and those stably expressing CytoATP indicators. Therefore, the same plate of cells was able to be utilized for comparative measurement of ATP via CTG immediately following the 2-hour time point in this study.

Color-scaled ATP Ratio images confirm that despite the difference in cell density, cytoplasmic ATP levels appear

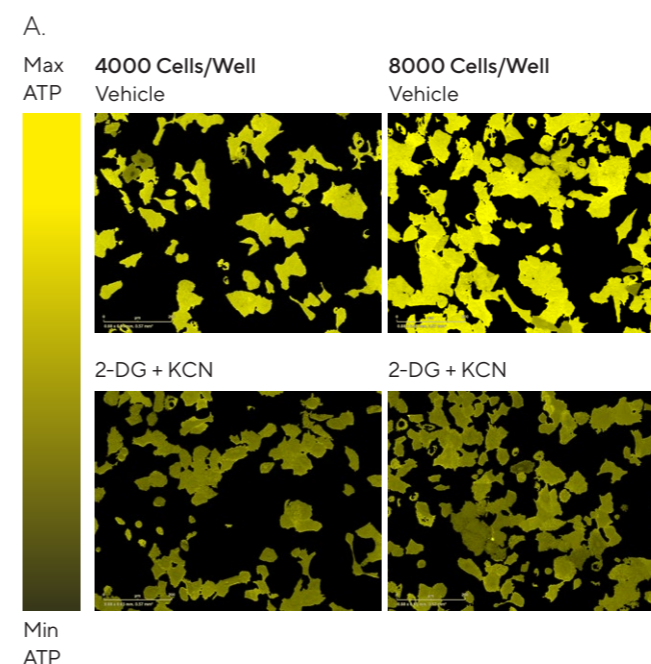


Figure 4: Ratiometric output enables measurement of ATP independent of cell number. Color-scaled ratio images of HeLa cells stably expressing CytoATP seeded at 4,000 or 8,000 cells per well and exposed to vehicle or 2-DG (20 mM) and KCN (2 mM) (A). Endpoint (2 h) measurement of ATP using Incucyte® ATP Assay is independent of cell number (B) while CellTiter-Glo® luminescence signal from the same cells depends on cell density (C).

similar between the two plating conditions, with vehicle-treated cells appearing brighter yellow than those treated with combined 2-DG and KCN in both cases (Figure 4A). Concentration-response curves were plotted from data collected at the 2-hour time point. Curves generated from the two plating densities via the Incucyte® ATP assay were overlaid, confirming that measurements were independent of cell number (Figure 4B). In contrast, CTG measurements taken from the higher (8,000 cells/well) density were consistently approximately 2-fold higher than those taken from the lower (4,000 cells/well) density across all drug treatment conditions (Figure 4C), consistent with the cell density dependence expected of this reagent. It is of note that although CTG is often used by researchers as a viability assay to estimate cell number, there was little difference in confluence between treatment groups across wells with the same cell plating density. For example, within the 4,000 cells/well group, confluence was 20.6% for vehicle-treated wells vs. 20.8% for 20 mM 2-DG + 2 mM KCN-treated wells. A slight decrease in confluence was observed at the highest treatment concentration, but this appeared to be due to a morphology change rather than cell death. Therefore, the differences in CTG values between drug treatments can be primarily attributed to lower ATP within the cells present, as supported by the Incucyte® ATP assay dataset.

## Qualitative Assessment of Cell Morphology

Traditional techniques often require destructive methods to measure changes in ATP and other metabolites of interest. Live-cell imaging and analysis offers the benefit of monitoring alterations in cell growth and morphology in tandem with ATP measurement without imparting a requirement for additional technology or concatenated end points. HD Phase images are collected at each time point in the Incucyte® ATP assay, enabling quantification of confluence and qualitative assessment of images to reveal morphological changes that accompany alterations in ATP. To exemplify this concept, we treated HeLa cells stably expressing CytoATP indicators with compounds exhibiting variable mechanisms of action: chlorpromazine (6.25–100  $\mu$ M), a dopamine D2 receptor antagonist, etoposide (0.14–100  $\mu$ M), a topoisomerase II inhibitor, and combined 2-DG (63  $\mu$ M–40 mM) + KCN (6.3  $\mu$ M–4 mM), mechanisms described above. In each case, two baseline scans were collected prior to drug treatment. All compounds induced a concentration-dependent depletion of ATP, but with a variable time of onset

ranging from within 20 minutes to > 24 h after administration (Figure 5, right column). The left column depicts HD Phase images collected at concentrations and time points corresponding to ATP < 20% of vehicle-treated values for each compound. Chlorpromazine treatment resulted in a small, rounded phenotype suggestive of apoptosis, consistent with its known cytotoxic profile. Following etoposide treatment, some cells demonstrated a similar rounded morphology to chlorpromazine, but many were enlarged and flattened, indicative of a senescence phenotype. Etoposide has previously been shown to induce a combination of apoptosis and senescence, consistent with the mixed morphology observed in this study<sup>7</sup>. In contrast, the morphology of combined 2-DG + KCN treated cells was remarkably similar to vehicle-treated cells at this concentration and time point. Thus, despite inducing similar reductions in ATP, drastic differences in morphology were observed between compounds with varying mechanisms of action.

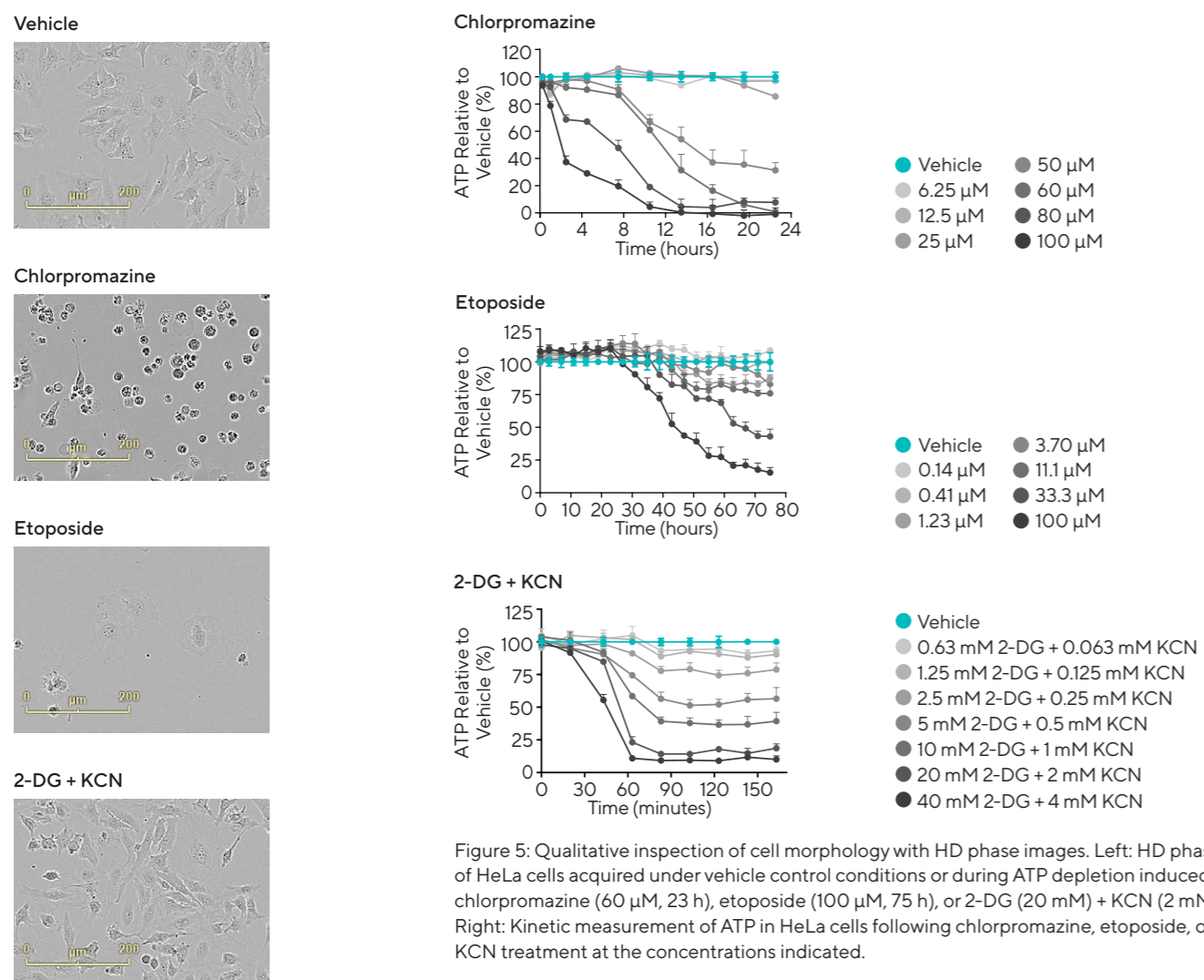


Figure 5: Qualitative inspection of cell morphology with HD phase images. Left: HD phase images of HeLa cells acquired under vehicle control conditions or during ATP depletion induced by chlorpromazine (60  $\mu$ M, 23 h), etoposide (100  $\mu$ M, 75 h), or 2-DG (20 mM) + KCN (2 mM) (80 min). Right: Kinetic measurement of ATP in HeLa cells following chlorpromazine, etoposide, or 2-DG + KCN treatment at the concentrations indicated.

## Effect of GLS-1 Inhibition on ATP in Mono- and Co-Culture Models

One of the most common and well-defined metabolic requirements of tumor cells is a dependence on glutamine, considered to be a non-essential amino acid for most normal cells. Glutamine serves diverse functions, including fueling mitochondrial ATP production by supplying  $\alpha$ -ketoglutarate to the TCA cycle. Therapeutic strategies targeting the supply and metabolic pathways of such conditionally essential amino acids have shown some clinical success<sup>8,9</sup> and continue to be an area of intense research. CB-839 (brand name Telaglenastat, Calithera Biosciences) is an inhibitor of glutaminase, the enzyme that catalyzes the first step in glutamine metabolism, and is currently in Phase 2 clinical trials for a variety of indications. In preclinical studies, CB-839 demonstrated a preferential anti-proliferative effect in triple-negative breast cancer (TNBC) lines compared to their receptor-positive counterparts<sup>10</sup>. Building upon these findings, the effect of CB-839 on ATP was characterized in both mono- and co-culture models using the Incucyte® ATP assay.

A panel of four TNBC (BT-20, HCC38, HCC1806, and MDA-MB-231) and four receptor-positive breast cancer (MCF7, ZR-75-1, AU565, and SKBR3) cell lines stably expressing CytoATP indicators were generated. The effect

of CB-839 (1.4 nM–1  $\mu$ M) on ATP was first evaluated in breast cancer cells cultured alone. CB-839 induced little to no effect on ATP of most receptor-positive cell lines, exemplified by results observed with ZR-75-1 cells (Figure 6A). The exception was MCF7 cells, which displayed a robust but transient depletion of ATP followed by full recovery within 48 h, highlighting the value of kinetic live-cell ATP measurements (Figure 6A). In contrast, CB-839 induced a concentration-dependent depletion of ATP that was sustained throughout the 72 h time course in the TNBC cell line MDA-MB-231 (Figure 6B). Similar results were observed across the panel of TNBC lines tested (Figure 7B–C). Incucyte® phase confluence measurements performed in tandem revealed that the sustained ATP depletion observed in MDA-MB-231 cells corresponded to a stronger anti-proliferative effect than the robust but transient ATP depletion in MCF7 cells. These data are consistent with previously published results demonstrating a modest but significant anti-proliferative effect of CB-839 in MCF7 cells<sup>10</sup>. Congruent with the established mechanism of CB-839, a similar trend was observed when cells were cultured in the absence of glutamine, with TNBC cell lines being more robustly affected (Figure 6C).

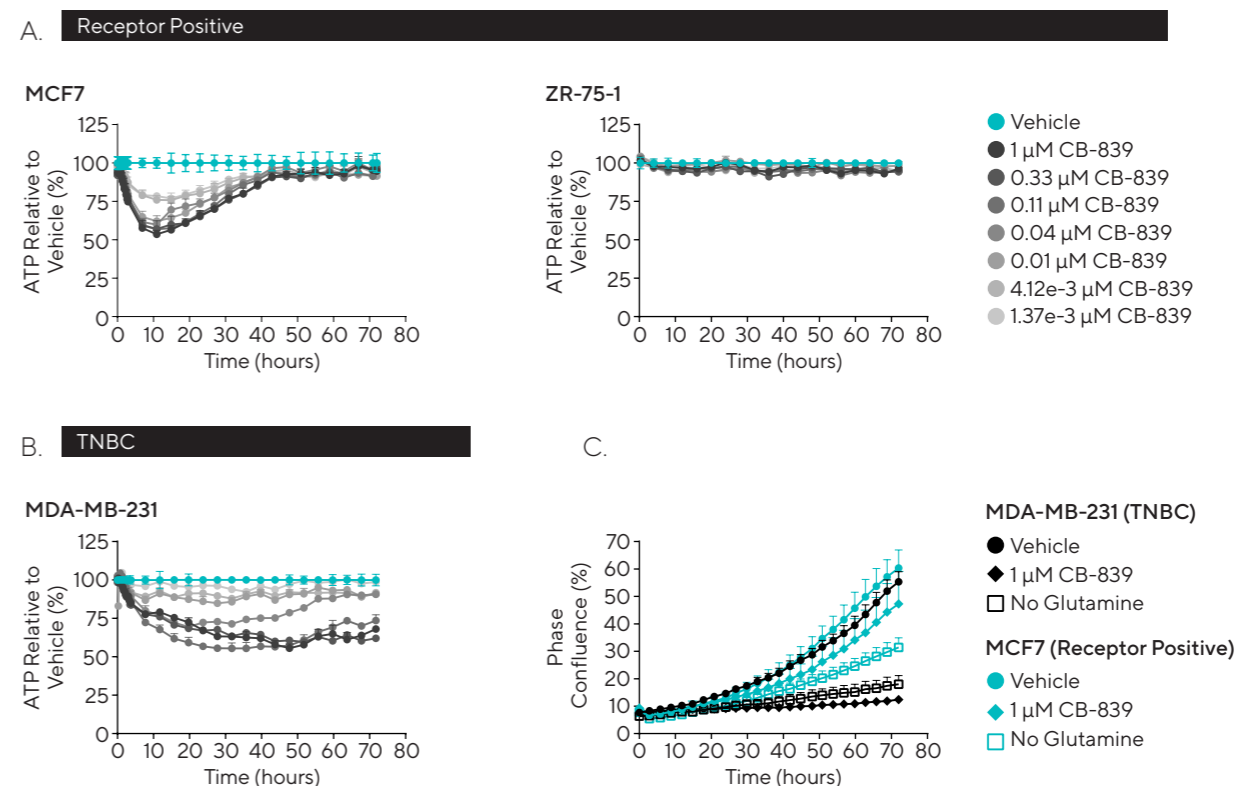


Figure 6: Differential effect of GLS-1 inhibition on ATP of receptor-positive and TNBC cell lines. Kinetic measurement of ATP following CB-839 treatment in receptor-positive breast cancer cell lines, MCF7 and ZR-75-1 (A) and TNBC cell line, MDA-MB-231 (B). Effect of 1  $\mu$ M CB-839 or glutamine deprivation on confluence measurements of MDA-MB-231 and MCF7 cells (C).

The effect of CB-839 on ATP was next evaluated in breast cancer cells co-cultured with CCD14086SK fibroblasts as a model of stromal-tumor cell nutrient exchange (Fig 7A). When HCC38 TNBC cells were cultured alone, CB-839 (1.4 nM–1  $\mu$ M) induced a sustained, concentration-dependent depletion of ATP, similar to the kinetic profile observed with MDA-MB-231 cells. When the same experiment was performed in the presence of CCD14086SK fibroblasts, HCC38 cells demonstrated an attenuated response to CB-839 (Figure 7B). Again, this observation was consistent across all TNBC lines. Concentration-response curves of data collected at the 72-hour time point demonstrate a similar separation between monoculture (solid lines) and co-culture responses

(dashed lines) across all TNBC cell lines tested (Figure 7C). In contrast, MCF7 cells displayed no difference between mono- and co-culture conditions. Unsurprisingly, the lack of CB-839 sensitivity observed in other receptor-positive lines was also unchanged in the presence of CCD14086SK cells. Figure 7D depicts 72-hour concentration-response curves for receptor-positive cell lines. In the case of MCF7 cells, the 15-hour time point was selected to highlight the overlapping concentration-response curves between mono- and co-culture (Figure 7D). These data are important because they demonstrate that metabolic exchange or another biological interaction with stromal cells, rather than drug buffering, promotes resistance to CB-839 in TNBC cells.

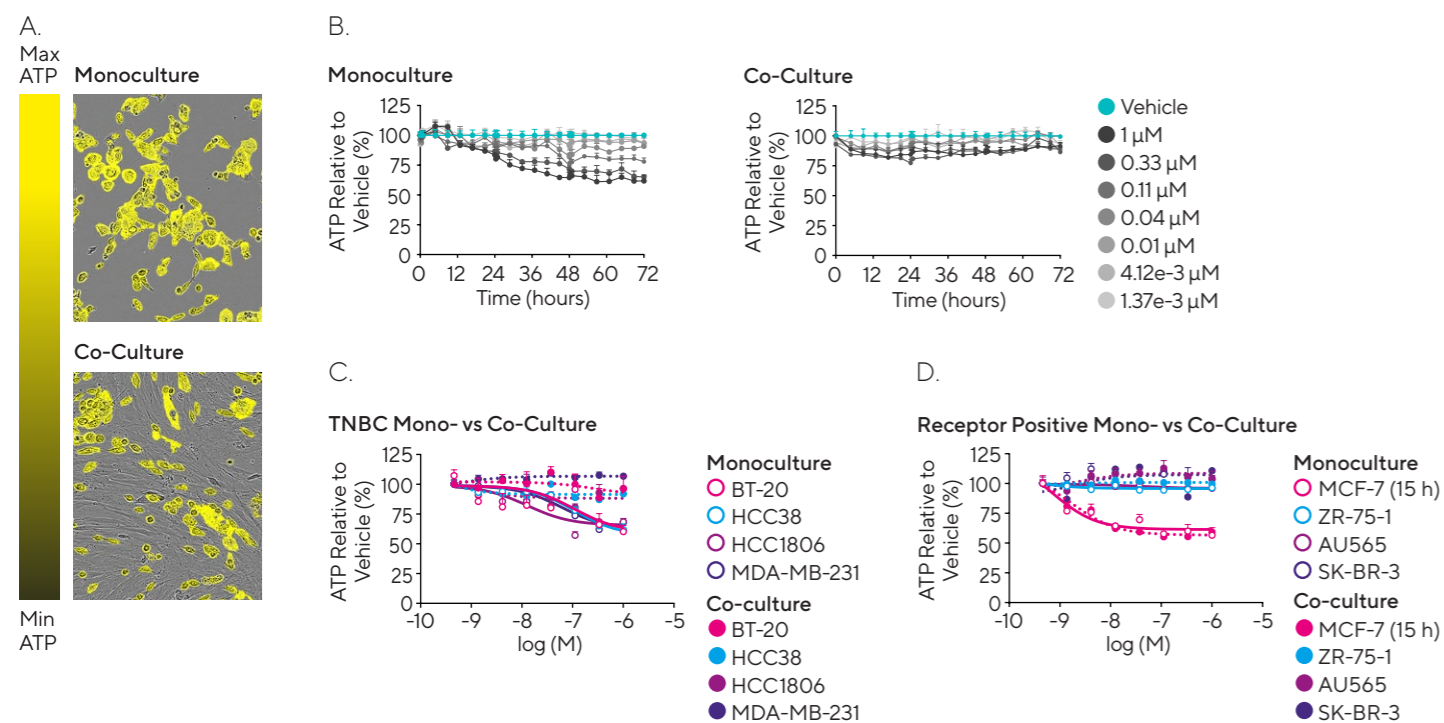


Figure 7: Effect of GLS-1 inhibition on ATP of breast cancer cells in co-culture. Color-scaled images provide visualization of ATP in HCC38 cells treated with 330 nM CB-839 in monoculture and in co-culture with CCD14086SK cells (A). Kinetic measurement of ATP in HCC38 (TNBC cell line) in monoculture and co-culture with CCD14086SK cells (B). Comparison of CB-839 concentration-response curves between a panel of TNBC (C) and receptor-positive breast cancer cell lines (D) in monoculture and co-culture. Data represent 72 h time point except where indicated.

## Assessment of Compound Effects on Mitochondrial Function

Due to its cytoplasmic localization, ATP produced by both glycolytic and mitochondrial OXPHOS pathways contributes to the pool measured by the Incucyte<sup>®</sup> CytoATP reporter. However, assessment of specific effects on mitochondrial bioenergetics is often of interest when performing mechanism of action studies. In addition, mitochondrial dysfunction is being increasingly recognized as an underlying cause of drug-induced liver injury (DILI), which is the most common adverse event for non-approval or withdrawal of drugs<sup>11</sup>. Because supraphysiological concentrations of glucose in standard cell culture media can often allow cells to increase glycolysis to compensate for a decrease in OXPHOS, mitochondrial-driven toxicity can be easily missed in many traditional assays. Replacement of glucose with galactose in cell culture media is an experimental strategy that can be utilized to uncover mitochondrial vulnerabilities. Unlike glucose, oxidation of galactose to pyruvate does not result in ATP production, resulting in increased reliance on OXPHOS and sensitivity to mitochondrial toxicants<sup>12</sup>. The effect of compounds with known toxicity profiles was evaluated utilizing a live-cell adaptation of this glucose-galactose switch experimental paradigm.

NIH 3T3 cells stably expressing Incucyte<sup>®</sup> CytoATP or Non-binding Control indicators were adapted to media containing galactose in place of glucose according to procedures described in the Incucyte<sup>®</sup> ATP Assay protocol<sup>4</sup>. Cells grown in galactose were plated alongside their glucose-grown counterparts for a direct comparison of compound-induced effects on CytoATP readout between the two media conditions. Following two baseline scans to confirm equal starting ATP values across treatment conditions, cells were treated with compounds previously shown in literature to be nontoxic, cytotoxic, or mitotoxic (0.4–100  $\mu$ M for all compounds). Images were acquired and analyzed every 20 min at early time points to capture early changes in ATP, then every hour from 3–24 h after compound addition to monitor responses for recovery, stability, or progressive depletion of ATP. Figure 8 displays representative datasets from each category.

As expected, the nontoxic compound ambrisentan<sup>13</sup> did not affect ATP at any concentration, regardless of cell culture media conditions (left column). The antipsychotic compound chlorpromazine, which carries a black box warning due to cardiovascular and other risks, induced a rapid, concentration-dependent depletion of ATP in cells grown in both glucose (top middle) and galactose (middle). Concentration-response curves generated from data collected at the 24-hour time point are shown in the bottom row. The overlapping curves between cells grown in glucose or galactose are indicative of a cytotoxic profile, consistent with previous results<sup>14</sup>. In contrast, the antidepressant nefazodone, which has been associated with DILI and shown to induce mitochondrial toxicity<sup>14</sup>, exhibited increased potency in cells grown in galactose. When cells were grown in glucose-containing medium, only the highest concentration (100  $\mu$ M) of nefazodone elicited a sustained, progressive depletion of ATP over time (top right). A small and transient depletion followed by recovery was also observed at the 50  $\mu$ M concentration. However, the same concentrations of nefazodone resulted in an almost immediate and robust depletion of ATP in galactose-grown cells. ATP continued to decrease to nearly undetectable levels over the course of the assay. At lower concentrations (12.5–25  $\mu$ M), galactose-grown cells exhibited a rapid, moderate decrease in ATP, partial recovery, then reversal and progressive depletion over the time course of the assay (middle right). Concentration-response curves also demonstrate variation in the relationship between responses elicited under glucose and galactose media conditions at different time points (bottom right). In each case, nefazodone EC<sub>50</sub> values were > 4-fold higher in cells grown in glucose compared to galactose-grown cells, consistent with a mitotoxic compound profile. These results demonstrate the utility of the Incucyte<sup>®</sup> ATP assay to characterize specific compound effects on OXPHOS.

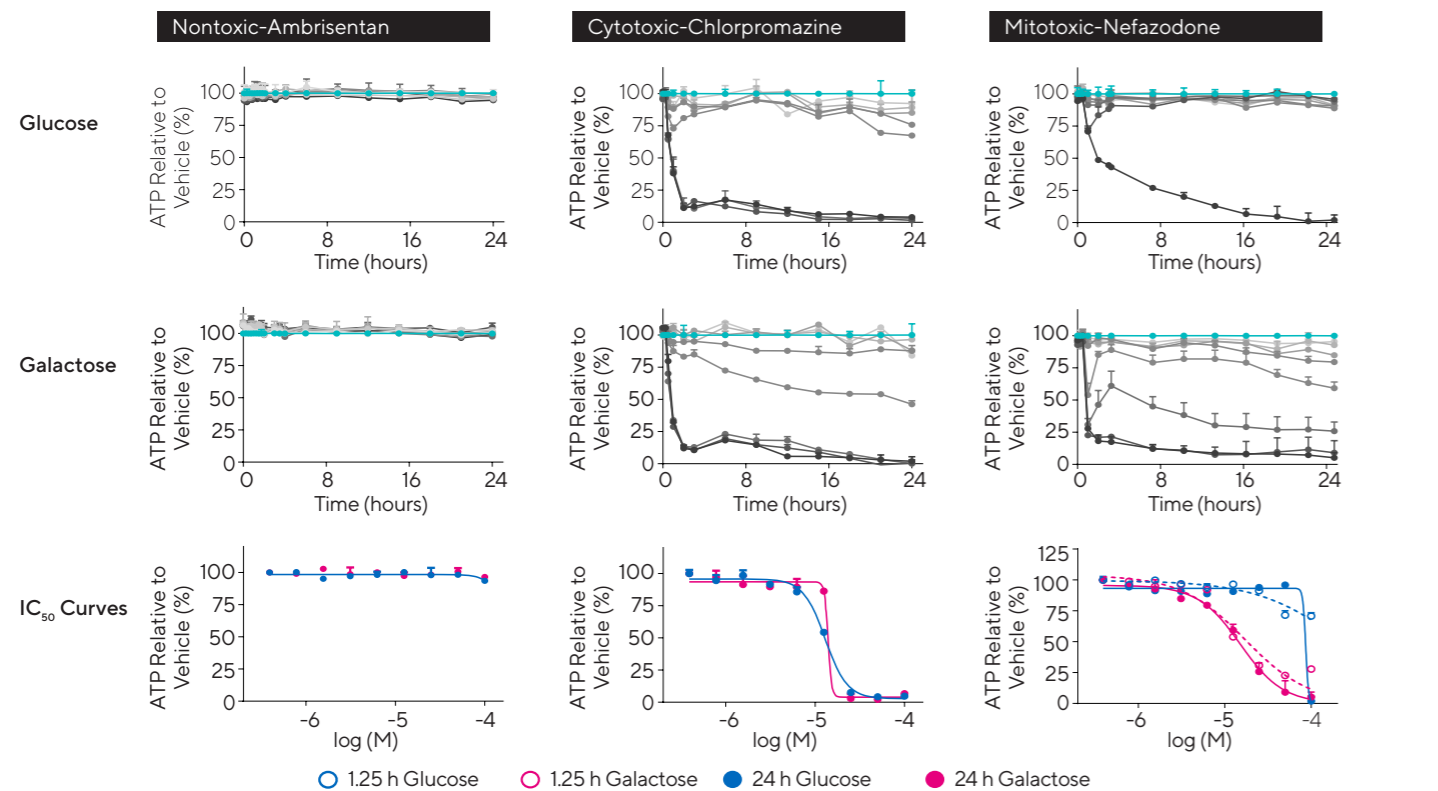


Figure 8: Glucose-galactose switch enables assessment of mitochondrial toxicity. Comparison of known nontoxic (ambrisentan, left column), cytotoxic (chlorpromazine, middle) and mitotoxic (nefazodone, right column) compound profiles. For each compound, effects on ATP were monitored in cells grown in glucose (top row) or galactose (middle row) over 24 h. ATP ratio values were normalized to respective vehicle controls for each time point. Concentration-response curves (bottom row) are depicted at the time points indicated. Consistent with expected profiles for each class, ambrisentan did not affect ATP, chlorpromazine depleted ATP to a comparable degree in both media conditions, and nefazodone exhibited substantially increased potency in galactose-grown cells.

## Summary and Outlook

In this application note, the unique features and utility of the Incucyte® ATP Assay have been highlighted. The novel, genetically-encoded Incucyte® CytoATP and Non-binding Control Lentiviral reagents combined with the ratiometric readouts, enabled by the Incucyte® SX5 Metabolism Optical Module and Incucyte® ATP Analysis Software Module, provide researchers with direct ATP measurements that are independent of cell number or reporter expression levels.

Glutaminase inhibition in breast cancer was utilized as an example to demonstrate how the Incucyte® ATP assay can be employed to characterize the efficacy, selectivity, and mechanisms of compounds that target cancer metabolism in mono- and complex co-culture models. Confluence and morphological changes can also be monitored via HD Phase images to provide additional assessment and

insight into compound effects. In addition, the Incucyte® ATP Assay was shown to provide a live-cell adaptation to the glucose-galactose switch paradigm, which can be used as a tool for screening for mitochondrial toxicity liabilities or for mechanistic studies of compounds to assess specific compound effects on mitochondrial bioenergetics. In both applications, dynamic changes in ATP were observed over the course of the assay, highlighting the value of a live-cell experimental approach to provide additional insight and guide end point selection for complementary assays. Metabolically-targeted treatments are the subject of intense investigation in the oncology field. There is a critical need for improved tools to advance our understanding of how nutrient exchange and other cell-cell interactions influence the efficacy of potential therapeutic strategies. The Incucyte® ATP Assay is uniquely positioned to enable researchers to answer these important questions.

## References

- Pavlova NN and Thompson, CB. **The Emerging Hallmarks of Cancer Metabolism.** *Cell Metabolism*, 23(1);27-47 (2016) 10.1016/j.cmet.2015.12.006
- Fiori ME, et al. **Cancer-associated fibroblasts as abettors of tumor progression at the crossroads of EMT and therapy resistance.** *BMC, Molecular Cancer*, 18(70) (2019) 10.1186/s12943-019-0994-2
- Milo R, et al. **BioNumbers—the database of key numbers in molecular and cell biology.** *Nucleic Acids Research*, 38(1);D750-D753 (2010)
- Essen BioScience. **Incucyte® CytoATP Product Guide.** <https://www.essenbioscience.com/media/uploads/files/CytoATP-Product-Guide-en-8000-0739-A00-L-Sartorius.pdf>. (2020)
- Wick, AN, et al. **Localization of the primary metabolic block produced by 2-deoxyglucose.** *Journal of Biological Chemistry*, 224(2);963-969 (1957)
- Wainio WW and Greenlees J. **Complexes of cytochrome c oxidase with cyanide and carbon monoxide.** *Archives of Biochemistry and Biophysics*, 90(1);18-21 (1960) 10.1016/0003-9861(60)90605-6
- Nagano T, et al. **Identification of cellular senescence-specific genes by comparative transcriptomics.** *Scientific Reports*, 6(1);1-13 (2016) 10.1038/srep31758
- Ascierto PA, et al. **Pegylated arginine deiminase treatment of patients with metastatic melanoma: Results from phase I and II studies.** *Journal of Clinical Oncology*, 23(30);7660-7668 (2005) 10.1200/JCO.2005.02.0933
- Avramis VI and Tiwari PN. **Asparaginase (native ASNase or pegylated ASNase) in the treatment of acute lymphoblastic leukemia.** *Int J Nanomedicine*, 1(3);241-254 (2006)
- Gross MI, et al. **Antitumor activity of the glutaminase inhibitor CB-839 in triple-negative breast cancer.** *Molecular Cancer Therapeutics*, 13(4);890-901 (2014) 10.1158/1535-7163.MCT-13-0870
- Kamalian L, et al. **The utility of HepG2 cells to identify direct mitochondrial dysfunction in the absence of cell death.** *Toxicology in Vitro*, 29(4);732-740 (2015) 10.1016/j.tiv.2015.02.011
- Marroquin LD, et al. **Circumventing the Crabtree effect: replacing media glucose with galactose increases susceptibility of HepG2 cells to mitochondrial toxicants.** *Toxicological sciences: an official journal of the Society of Toxicology*, 97(2);539-47 (2007) 10.1093/toxsci/kfm052
- National Institute of Diabetes and Digestive and Kidney Diseases. **LiverTox: Clinical and Research Information on Drug-Induced Liver Injury.** <https://pubmed.ncbi.nlm.nih.gov/31643176/> (updated 2020)
- Sanuki Y, et al. **A rapid mitochondrial toxicity assay utilizing rapidly changing cell energy metabolism.** *Journal of Toxicological Sciences*, 42(3);349-358 (2017) 10.2131/jts.42.349

# Sales and Service Contacts

For further contacts, visit  
[www.sartorius.com](http://www.sartorius.com)

## **Essen BioScience, A Sartorius Company**

[www.sartorius.com/incucyte](http://www.sartorius.com/incucyte)

E-Mail: [AskAScientist@sartorius.com](mailto:AskAScientist@sartorius.com)

### **North America**

Essen BioScience Inc.  
300 West Morgan Road  
Ann Arbor, Michigan, 48108  
USA  
Telephone +1 734 769 1600  
E-Mail: [orders.US07@sartorius.com](mailto:orders.US07@sartorius.com)

### **APAC**

Essen BioScience K.K.  
4th Floor Daiwa Shinagawa North  
Bldg.  
1-8-11 Kita-Shinagawa  
Shinagawa-ku, Tokyo  
140-0001  
Japan  
Telephone: +81 3 6478 5202  
E-Mail: [orders.US07@sartorius.com](mailto:orders.US07@sartorius.com)

### **Europe**

Essen BioScience Ltd.  
Units 2 & 3 The Quadrant  
Newark Close  
Royston Hertfordshire  
SG8 5HL  
United Kingdom  
Telephone +44 1763 227400  
E-Mail:  
[euorders.UK03@sartorius.com](mailto:euorders.UK03@sartorius.com)

Specifications subject to change without notice.

© 2020. All rights reserved. Incucyte, Essen BioScience, and all names of Essen BioScience products are registered trademarks and the property of Essen BioScience unless otherwise specified.

Essen BioScience is a Sartorius Company. Publication No.: 8000-0749-A00

Status: 09 | 2020